CHAPTER 25

Control Approach to Fictitious-Domain Methods Application to Fluid Dynamics and Electro-Magnetics

C. Atamian*
Q. V. Dinh*
R. Glowinski†
Jiwen He*
J. Périaux*

1. Introduction and Motivation

Research on *Fictitious Domain Methods for Partial Differential Equations* has always been active, particularly in U.S.S.R. (cf. e.g. [1]-[3]) and the references therein), but also in the West (cf. e.g., [4], [5]), motivated mostly by the solution of linear elliptic equations. More recently, these methods have been successfully applied by Boeing Airplane Co. (cf. ref. [6]) for the numerical simulation of transonic flow around actual aircrafts such as the Boeing 747 and the F-16, including flow around and/or inside air intakes, loads at wing tips, external fuel tanks, etc...

Indeed Boeing research engineers apply also these techniques for accoustics and electromagnetic calculations via the solution of the Helmholtz and Maxwell equations.

The reasons of that persistence of fictitious domain methods, and in fact of their increased use in industrial applications, are that at the expense of some mathematical sophistication they allow the numerical solution of problems in complicated geometries by methods operating on a simple geometry domain containing the complicated one. This gives access to a combination of simple approximation methods, well suited to rectangles and boxes (finite differences, low order finite element on regular meshes, spectral methods, wavelets, ...), with efficient solution methods such as Fast Fourier Transform, Fast Poisson and Helmzholtz solvers, multigrid, ... The resulting methodology is highly vectorizable and parallelizable, and also well suited to fast domain decomposition methods.

*Dassault Industry, France.
†Mathematics Department, University of Houston.

In this method-oriented paper, we would like to discuss an implementation of fictitious domain methods which is based on an *optimal control formulation* leading to problems very close to those discussed in J. L. Lions [7]. This approach has very definite advantages since it is based on a *least-squares formulation* of the boundary condition to be satisfied on the actual boundary; it is then naturally suited for iterative methods such as conjugate gradient, GMRES, etc... The preliminary results which have been obtained are encouraging, and there is indeed a large room for improvement, including the investigation of preconditioners more efficient than those presently used which may be slow in some occasions (some variants are precisely discussed in [8]).

An outline of this report is the following:

In Section 2, we shall consider the solution of simple model problems such as the Poisson problem for the Laplace operator with Dirichlet and Neumann boundary conditions.

In Section 3, we shall discuss the solution of the Helmholtz equations by control and fictitious domain methods.

Finally, in Section 4, we shall present the results of numerical experiments using the methodology discussed in Sections 2 and 3.

2. Solution of the Poisson Equation for Dirichlet and Neumann Boundary Conditions. Applications

2.1 Formulation of the model problem

Motivated by Fluid Dynamics, we consider the situation depicted on Figure 2.1 where

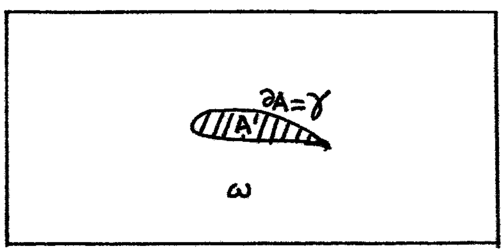

Figure 2.1

(2.1) $\Omega = \textit{interior of the closure of } \omega \cup A, \ \gamma = \partial A, \ \Gamma = \partial\Omega,$

the domain A being, for example, an airfoil.

The basic problems that we want to solve are the *Poisson-Dirichlet problem*

(2.2) $-\Delta\varphi = f \textit{ in } \omega, \ \varphi = g \textit{ on } \gamma\cup\Gamma,$

and the *Poisson-Neumann problem*

(2.3) $-\Delta\varphi = f \textit{ in } \omega, \ \dfrac{\partial\varphi}{\partial n} = g \textit{ on } \gamma\cup\Gamma.$

Concerning problem (2.3) we shall assume that the following *compatibility condition*

(2.4) $\int_\omega f dx + \int_{\gamma\cup\Gamma} g d\sigma = 0$

is satisfied, implying that the above problem has a unique solution in $H^1(\omega)/\mathbf{R}$, (i.e. is uniquely defined within to an arbitrary additive constant).

2.2 A control method for the Poisson-Dirichlet problem

2.2.1 An equivalent control formulation of problem (2.2)

Let's denote by $J(\cdot)$ the functional defined by

(2.5) $J(v) = \frac{1}{2}\int_\gamma |y(v) - g_\gamma|^2 + \frac{r}{2}\int_\omega |f - v|^2 dx,$

where in (2.5), we have

(i) $g_\gamma = g|_\gamma,$

(ii) $r \geq 0,$

(iii) y(v) defined as the solution of the following Dirichlet problem over the larger domain Ω:

$(2.6)_1$ $$-\Delta y = v \textit{ in } \Omega,$$

$(2.6)_2$ $$y = g_\Gamma \textit{ on } \Gamma,$$

with $g_\Gamma = g|_\Gamma$.

Concerning the set $\mathcal{U}_f$ where the minimization will take place, we have two natural choices:

1st choice: If $r=0$, we shall take

(2.7) $$\mathcal{U}_f = \{v | v \in L^2(\Omega),\ v = f \textit{ on } \omega\}.$$

2nd choice: If $r>0$, we can take

(2.8) $$\mathcal{U}_f = L^2(\Omega).$$

We clearly have the following

Theorem 2.1: *Suppose that* $f \in L^2(\omega)$ *and that* $g \in H^{\frac{1}{2}}(\gamma \cup \Gamma)$, *then the control problem*

(2.9) $$\begin{cases} u \in \mathcal{U}_f, \\ J(u) \leq J(v),\ \forall v \in \mathcal{U}_f, \end{cases}$$

is equivalent to the Poisson-Dirichlet problem (2.2); we also have in the two above cases $u|_\omega = f$, and also $y|_\omega$ is the solution of the problem (2.2). □

The functional $J(\cdot)$ is clearly C^∞ over $L^2(\Omega)$; it is also *convex*, and therefore (cf. e.g. [7]) the solution of (2.9) has to satisfy

(2.10)
$$\begin{cases} u\in\mathcal{U}_f, \\ (J'(u), v-u) \geq 0, \ \forall v\in\mathcal{U}_f, \end{cases}$$

where in (2.10), $(\cdot,\cdot)$ denotes the usual scalar product of $L^2(\Omega)$, and J' is the differential of J.

The practical solution of (2.9), (2.10) will be based on either conjugate gradient, or GMRES type algorithms, combined to finite element approximations; it is therefore of major importance to compute $J'(v)$ for $v\in L^2(\Omega)$.

Remark 2.1: Other approaches using optimization techniques can be used to construct fictitious domain methods for the Poisson-Dirichlet problem (2.2); one of them is discussed in [8].

2.2.2 Calculation of J'

Let's δv be a "small" variation of v; we clearly have

(2.11)
$$\delta J(v) = (J'(v),\delta v) = \int_\gamma (y-g_\gamma)\delta y d\gamma + r\int_\omega (v-f)\delta v dx,$$

with δy the solution of

(2.12)
$$-\Delta\delta y = \delta v \ \textit{in}\ \Omega,\ \delta y = 0 \ \textit{on}\ \Gamma.$$

The *variational formulation* of (2.12) is given by

(2.13)
$$\begin{cases} \delta y\in H_0^1(\Omega), \\ \int_\Omega \nabla\delta y\cdot\nabla z dx = \int_\Omega \delta v z dx, \forall z\in H_0^1(\Omega). \end{cases}$$

Define then p as the solution of

(2.14)
$$\begin{cases} p\in H_0^1(\Omega), \\ \int_\Omega \nabla p\cdot\nabla z dx = \int_\gamma (y-g_\gamma)z d\gamma,\ \forall z\in H_0^1(\Omega). \end{cases}$$

Taking $z=p$ in (2.13) and $z=\delta y$ in (2.14), we obtain by comparison that

(2.15)
$$\int_\gamma (y-g_\gamma)\delta y d\gamma = \int_\Omega p\delta v dx,$$

which implies in turn

(2.16)
$$J'(v) = p + r(v-f)|_\omega.$$

2.2.3 Conjugate Gradient Solution of Problem (2.9)

Problem (2.9) can be solved by a conjugate gradient algorithm, with $\mathcal{U}_f$ defined by either (2.7) or (2.8).

We first consider the second case since it is the simpler one.

A. Description of the conjugate gradient algorithm if $\mathcal{U}_f=L^2(\Omega)$:

Initialization:

(2.17) $u^o\in L^2(\Omega)$ *is given;*

solve the Dirichlet problems

(2.18)
$$-\Delta y^o = u^o \textit{ in } \Omega,\ y^o = g_\Gamma \textit{ on } \Gamma,$$

and

$$(2.19)\qquad \begin{cases} p^o \in H_0^1(\Omega), \\ \int_\Omega \nabla p^o \cdot \nabla z dx = \int_\gamma (y^o - g_\gamma) z d\gamma, \ \forall z \in H_0^1(\Omega). \end{cases}$$

Define

$$(2.20)\qquad g^o = p^o + r(u^o - f)|_\omega,$$

and

$$(2.21)\qquad w^o = g^o. \qquad \square$$

Then for $n \geq 0$, *assuming that* u^n, y^n, g^n and w^n *are known we update them as follows:*

Descent: *Solve*

$$(2.22)\qquad -\Delta \overline{y}^n = w^n \ \textit{in}\ \Omega,\ \overline{y}^n = 0 \ \textit{on}\ \Gamma,$$

and

$$(2.23)\qquad \begin{cases} \overline{p}^n \in H_0^1(\Omega) \\ \int_\Omega \nabla \overline{p}^n \cdot \nabla z dx = \int_\gamma \overline{y}^n z d\gamma, \ \forall z \in H_0^1(\Omega). \end{cases}$$

Compute then

$$(2.24)\qquad \rho_n = \frac{\int_\Omega |g^n|^2 dx}{\int_\Omega \overline{p}^n w^n dx + r \int_\omega |w^n|^2 dx}$$

and

(2.25) $$u^{n+1} = u^n - \rho_n w^n,$$

(2.26) $$y^{n+1} = y^n - \rho_n \bar{y}^n,$$

(2.27) $$g^{n+1} = g^n - \rho_n(\bar{p}^n + rw^n|_\omega).$$

Testing the convergence and constructing the new descent direction:

If $\|g^{n+1}\|_{L^2(\Omega)}/\|g^o\|_{L^2(\Omega)} \leq \epsilon$ *take* $u = u^{n+1}$, $y = y^{n+1}$; *if not compute*

(2.28) $$\gamma_n = \frac{\|g^{n+1}\|^2_{L^2(\Omega)}}{\|g^n\|^2_{L^2(\Omega)}},$$

and set

(2.29) $$w^{n+1} = g^{n+1} + \gamma_n w^n.$$ □

Do n=n+1 *and go to* (2.22).

We observe that the above algorithm requires the solution of two Dirichlet problems on Ω at each iteration.

B. Description of the conjugate gradient algorithm if $\mathcal{U}_f$ is given by (2.7)

It follows from (2.16) that if $\mathcal{U}_f$ is given by (2.7), then the optimality condition (2.10) reduces to

(2.30) $$\int_A p v dx = 0, \ \forall v \in L^2(A)$$

(we recall that $A = \Omega \backslash \bar{\omega}$).

In the present case we have to modify algorithm (2.17)-(2.29) as follows:

(i) *Replace* (2.17) *by:*

(2.31) $$u^o \in \mathcal{U}_f = \{v | v \in L^2(\Omega),\ v = f \text{ on } \omega\}.$$

(ii) *Replace* (2.20) *by:*

(2.32) $$g^o = p^o \chi_A$$

(*where* χ_A = *characteristic function* of A).

(iii) *Replace* (2.24) *by:*

(2.33) $$\rho_n = \frac{\int_A |g^n|^2 dx}{\int_A \bar{p}^n w^n dx}.$$

(iv) *Replace* (2.27) *by:*

(2.34) $$g^{n+1} = g^n - \rho_n \bar{p} n \chi_A.$$

(v) *If* $\|g^{n+1}\|_{L^2(A)} / \|g^o\|_{L^2(A)} \le \epsilon$ *take* $u = u^{n+1}$, $y = y^{n+1}$; *if not compute*

(2.35) $$\gamma_n = \frac{\|g^{n+1}\|^2_{L^2(A)}}{\|g^n\|^2_{L^2(A)}}.$$ □

The numerical results presented in Section 4 have been obtained using $\mathcal{U}_f$ defined by (2.7).

2.3 A Control Method for the Poisson-Neumann Problem.

2.3.1 Synopsis

We consider now a fictitious domain approach for the *Poisson-Neumann problem*, (2.3), namely

$$-\Delta\varphi = f \text{ in } \omega, \frac{\partial\varphi}{\partial n} = g \text{ on } \gamma\cup\Gamma. \tag{2.36}$$

A different, but in fact very related approach is discussed in ref. [8].

2.3.2 An equivalent control formulation of problem (2.36)

We denote by $J(\cdot)$ the functional defined by

$$J(v) = \frac{1}{2}\int_\gamma |\frac{\partial y}{\partial n} - g_\gamma|^2 d\gamma, \tag{2.37}$$

where, in (2.37), we have:

$$g_\gamma = g|_\gamma, \tag{2.38}$$

and $y(=y(v))$ defined as the solution of

$$(2.39)_1 \qquad -\Delta y = v \text{ in } \Omega,$$

$$(2.39)_2 \qquad \frac{\partial y}{\partial n} = g_\Gamma \text{ on } \Gamma,$$

with $g_\Gamma = g|_\Gamma$. In (2.37), (2.39) (and in the sequel) $\frac{\partial}{\partial n}$ denotes the outward normal derivative at ω.

We observe that in order to have problem (2.39) well-posed (within to an arbitrary additive constant) the following *compatibility condition*

$$\int_\Omega v dx + \int_\Gamma g_\Gamma d\Gamma = 0, \tag{2.40}$$

has to hold.

Concerning the set $\mathcal{U}_f$ where the minimization will take place, we limit ourselves to

$$(2.41) \qquad \mathcal{U}_f = \{v|v\in L^2(\Omega),\ v=f \textit{ on } \omega, \textit{ relation } (2.40) \textit{ is satisfied}\}.$$

Assuming that $f\in L^2(\omega)$, the above formulation makes sense, since the solution y of (2.39) will belong to $H^1(\Omega)$, implying in turn that $\frac{\partial y}{\partial n}|_\gamma \in H^{\frac{1}{2}}(\gamma)$.

The control problem to be associated to the boundary value problem (2.36) is therefore defined by

$$(2.42) \qquad \begin{cases} u\in\mathcal{U}_f, \\ J(u) \leq J(v),\ \forall v\in\mathcal{U}_f. \end{cases}$$

Problem (2.42) is *equivalent* to problem (2.36).

The above formulation which is quite natural leads however to difficulties concerning its practical implementation with C^o-conforming Lagrange finite elements. This is mostly due to the fact that $L^2(\gamma)$ is not a very appropriate trace space for $\frac{\partial y}{\partial n}$, implying technical difficulties in the calculation of J'. A systematic way to overcome the above difficulties is to approximate - at the discrete level - $\frac{\partial y}{\partial n}$ via Green's formula. The corresponding method is discussed in the following Section 2.3.3.

2.3.3 A finite element implementation of the control method.

We suppose for simplicity that A, ω and Ω are subsets of $\mathbf{R}^2$ and also that Ω is a polygonal domain. We introduce next a standard triangulation $\mathcal{T}_h$ of Ω and approximate $H^1(\Omega)$ by

$$(2.43) \qquad V_h = \left\{z_h|z_h\in C^o(\overline{\Omega}),\ z_h|_T\in P_1,\ \forall T\in\mathcal{T}_h\right\},$$

with P_1 = space of the polynomials in two variables of degree ≤ 1. Next, we approximate problem (2.39) by the following discrete linear variational problem

(2.44)
$$\begin{cases} y_h \in V_h; \ \forall z_h \in V_h, \ \textit{we have} \\ \int_\Omega \nabla y_h \cdot \nabla z_h dx = \int_\Omega v_h z_h dx + \int_\Gamma g_{h\Gamma} z_h d\Gamma, \end{cases}$$

with $g_{h\Gamma}$ an appropriate approximation of g_Γ, and $v_h \in \mathcal{U}_{hf}$, $\mathcal{U}_{hf}$ being an approximation of $\mathcal{U}_f$ contained in V_h.

To force (in some approximate way) $\frac{\partial y}{\partial n} - g_\gamma$ to be zero we use in fact a *method of moment.* In the continuous case, we have (from Green's fomula):

(2.45)
$$\begin{cases} \int_\gamma (\frac{\partial y}{\partial n} - g_\gamma) z d\gamma = -\int_\omega (\nabla y \cdot \nabla z + \Delta y z) dx - \int_\gamma g_\gamma z d\gamma \\ = -\int_\omega (\nabla y \cdot \nabla z - vz) dx - \int_\gamma g_\gamma z d_\gamma, \ \forall z \in H_o^1(\Omega); \end{cases}$$

we have, similarly (cf. Figure 2.1)

(2.46)
$$\begin{cases} \int_\gamma (\frac{\partial y}{\partial n} - g_\gamma) z d\gamma = -\int_A (\nabla y \cdot \nabla z + \Delta y z) dx - \int_\gamma g_\gamma z d\gamma \\ = -\int_A (\nabla y \cdot \nabla z - vz) dx - \int_\gamma g_\gamma z d_\gamma, \ \forall z \in H_o^1(\Omega). \end{cases}$$

In the discrete case, we use (2.45) and (2.46) as guidelines, as follows:

(i) We order from 1 to N_γ those basis functions w_i of V_h whose support interesect γ, as shown in Figure 2.2 below

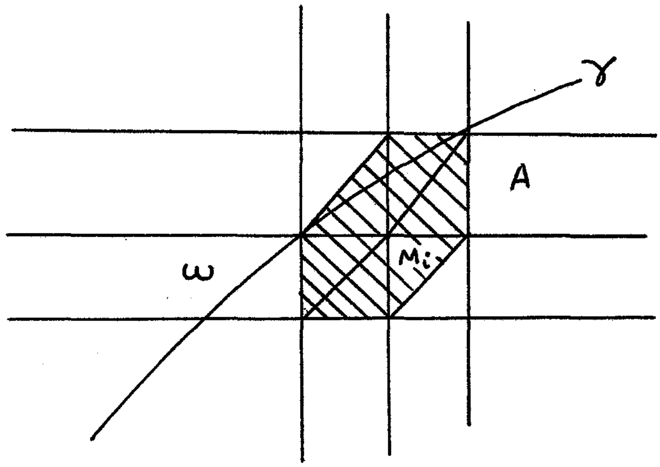

Figure 2.2

where (for example)$M_i \in A$. We have therefore $\int_{\gamma_i} d\gamma > 0$, with $\gamma_i = \gamma \cap \text{supp}(w_i)$ and also $w_i(M_j) = \delta_{ij}$, $\forall M_j$ vertex of $\mathcal{T}_h$.

We observe that for h small enough, M_i is close to γ if $i=1, \ldots, N_\gamma$.

(ii) To $i=1, \ldots, N_\gamma$ we associate the residual R_i defined by

$$R_i = \int_\omega (\nabla y_h \cdot \nabla w_i - v_h w_i)dx - \int_A (\nabla y_h \cdot \nabla w_i - v_h w_i)dx - 2\int_\gamma g_{\gamma h} w_i d\gamma, \tag{2.47}$$

where, in (2.47), $g_{\gamma h}$ is an approximation of g_γ. The discrete control problem is then discretized as follows:

$$\begin{cases} u_h \in \mathcal{U}_{hf}, \\ J_h(u_h) \le J_h(v_h), \ \forall v_h \in \mathcal{U}_{hf}, \end{cases} \tag{2.48}$$

with

$$(2.49)\qquad J_h(v_h) = \frac{1}{2}\sum_{i=1}^{N_\gamma} \alpha_i R_i^2,$$

where the α_i are positive coefficients (if $\mathcal{T}_h$ is a regular triangulation (like in Figure 2.2), we shall take $\alpha_i=1$, $\forall i$); in (2.49), the R_i are given by (2.47) with y_h the solution of (2.44).

Problem (2.48) can be solved by conjugate gradient techniques. An important step is again the knowledge of the gradient of the cost function, $J_h(\cdot)$.

We have then, from (2.49), (2.47),

$$(2.50)\qquad \begin{cases} J_h = (J_h'(v_h), \delta v_h) = \sum_{i=1}^{N_\gamma} \alpha_i R_i \delta R_i \\[2ex] = \sum_{i=1}^{N_\gamma} \alpha_i R_i \int_\omega (\nabla\delta y_h\cdot\nabla w_i - \delta v_h w_i)dx - \sum_{i=1}^{N_\gamma} \alpha_i R_i \int_A (\nabla\delta y_h\cdot\nabla w_i - \delta v_h w_i)dx \\[2ex] = \int_\omega (\nabla\delta y_h\cdot\nabla R_h - \delta v_h R_h)dx - \int_A (\nabla\delta y_h\cdot\nabla R_h - \delta v_h R_h)dx, \end{cases}$$

where, in (2.50), R_h is the element of V_h defined by

$$(2.51)\qquad R_h = \sum_{i=1}^{N_\gamma} \alpha_i R_i w_i$$

Relation (2.44) implies that δy_h is solution of

$$(2.52)\qquad \begin{cases} \delta y_h \in V_h, \\[1ex] \int_\Omega \nabla\delta y_h\cdot\nabla z_h dx = \int_\Omega \delta v_h z_h dx, \ \forall z_h \in V_h. \end{cases}$$

We introduce now the *adjoint equation*

$$(2.53)\quad \begin{cases} p_h \in V_h, \\ \int_\Omega \nabla p_h \cdot \nabla z_h dx = \int_\omega \nabla R_h \cdot \nabla z_h dx - \int_A \nabla R_h \cdot \nabla z_h dx, \ \forall z_h \in V_h. \end{cases}$$

Taking $z_h = p_h$ (resp. $z_h = \delta y_h$), in (2.52) (resp. (2.53)), we obtain, from (2.50) that

$$\delta J_h = (J_h'(v_h), \delta v_h) = \int_\Omega p_h \delta v_h dx - \int_\omega R_h \delta v_h dx + \int_A R_h \delta v_h dx,$$

which implies in turn that

$$(2.54)\quad \begin{cases} (J_h'(v_h), z_h) = \int_\Omega p_h z_h dx - \int_\omega R_h z_h dx + \int_A R_h z_h dx, \\ = \int_\Omega (p_h + (\chi_A - \chi_\omega) R_h) z_h dx, \ \forall z_h \in V_h. \end{cases}$$

Deriving a conjugate gradient algorithm solving (2.48), via (2.54), is straightforward, since it follows closely Section 2.2.3.

In Section 4, we shall present numerical results obtained from applying the above methodology to flow problems such as Neumann or Dirichlet associated to two-dimensional flow around a cylinder or a NACA0012 airfoil.

3. Application of control/fictitious domain methods to the solution of the Helmholtz equation

3.1 Formmulation of a relevant problem from acoustics.

We consider the scattering of a monochromatic wave (of wave number k) by an obstacle $A(\subset \mathbf{R}^3)$ of boundary γ. The reflected field satisfies the following *Helmholtz equation*

(3.1) $$-\Delta y - k^2 y = 0 \text{ in } \mathbf{R}^3 \backslash \bar{A},$$

(3.2) $$y = g \text{ on } \gamma,$$

(3.3) $$\lim_{r \to +\infty} \left(\frac{\partial y}{\partial r} - iky\right) = 0(1/r);$$

relation (3.3) is the classical *Sommerfeld radiation condition.*

3.2 A control/fictitious domain formulation of problem (3.1)-(3.3).

We denote by $J(\cdot)$ the functional defined by

(3.4) $$J(v) = \frac{1}{2}\int_{\gamma} |y-g|^2 d\gamma,$$

where, in (3.4), y is the solution of

(3.5) $$-\Delta y - k^2 y = v \text{ in } \mathbf{R}^3,$$

completed by the radiation condition (3.3).

We substitute then to problem (3.1)-(3.3) the control problem

(3.6) $$\begin{cases} \textit{Find } u \in \mathcal{U} \textit{ such that} \\ J(u) \le J(v), \ \forall v \in \mathcal{U}, \end{cases}$$

where

(3.7) $$\mathcal{U} = \{v | v \in L^2(\mathbf{R}^3), v = 0 \text{ in } \mathbf{R}^3 \backslash \bar{A}\}$$

($\mathcal{U}$ is clearly *isomorphic* to $L^2(A)$).

Remark 3.1: In this section, we consider *complex valued* functions. □

As in the previous Section 2, the practical solution of the control problem under consideration is greatly facilitated by the knowledge of the gradient of the cost function. The calculation of J' is addressed in the following Section 3.3.

3.3 Calculation of J'.

It can be shown that $J'(v)$ is defined by

$$(3.8) \qquad (J'(v),w) = \int_{\mathbf{R}^3} pwdx, \ \forall w \in L^2(\mathbf{R}^3),$$

with p the solution of the *adjoint equation*

$$(3.9) \qquad -\Delta p - k^2 p = 0 \text{ in } A \cup \omega$$

(here $\omega = \mathbf{R}^3 \backslash \bar{A}$), and with obvious notation,

$$(3.10) \qquad \left(\frac{\partial p}{\partial n_\omega} + \frac{\partial p}{\partial n_A}\right)\Big|_\gamma = (y - g)|_\gamma,$$

completed by the Sommerfeld radiation condition

$$(3.11) \qquad \lim_{r \to +\infty} \left(\frac{\partial p}{\partial r} + ikp\right) = 0(1/r).$$

If $\mathcal{U}$ is defined by (3.7), relation (3.8) clearly reduces to

$$(3.12) \qquad (J'(v),w) = \int_A pwdx, \ \forall w \in \mathcal{U}.$$

In the following Section 3.4, we shall discuss the more practical situation where the computational domain is bounded and where an *absorbing boundary condition* is prescribed on the external boundary.

3.4 Control formulation of the Helmholtz equation on bounded domains with an absorbing boundary condition.

A classical approach to the practical solution of the Helmholtz problem (3.1)-(3.3) is to substitute to the physical domain $\omega (= \mathbf{R}^3 \backslash \bar{A})$ a bounded one - still denoted ω - as shown in Figure 3.1, below

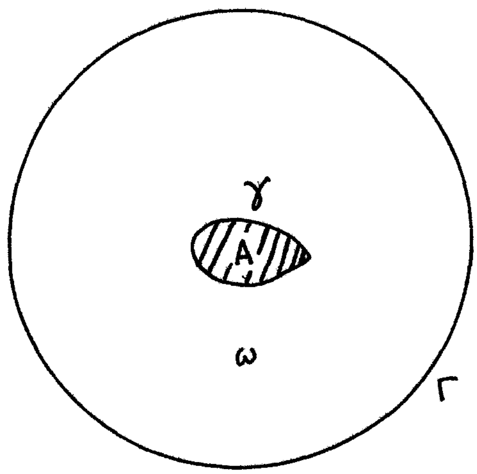

Figure 3.1

and to approximate the Sommerfeld radiation condition at infinity by a well-chosen *absorbing boundary condition* on Γ.

For simplicity, we shall suppose that Γ is smooth, as shown in Figure 3.1.

3.4.1 Formulation of the scattering problem and of the corresponding control problem.

Following [9], [10], we prescribe on Γ the second order absorbing boundary condition given by

(3.13) $$(\frac{\partial}{\partial n} - ik + \frac{i}{2k}\Delta_\Gamma)y = 0 \text{ on } \Gamma,$$

where

(3.14) Δ_Γ *is the Laplace-Beltrami operator.*

The Helmholtz problem to be solved is therefore

(3.15) $\qquad -\Delta y - k^2 y = 0 \textit{ in } \omega,$

(3.16) $\qquad y = g \textit{ on } \gamma,$

completed by (3.13).

The associated control formulation is given by

(3.17) $$\begin{cases} \textit{Find } u \in \mathcal{U} \textit{ such that} \\ J(u) \leq J(v), \ \forall v \in \mathcal{U}, \end{cases}$$

with $J(\cdot)$ still defined by

(3.18) $$J(v) = \frac{1}{2}\int_\gamma |y - g|^2 d\gamma,$$

with - this time - y defined by the solution of the boundary value problem

(3.19) $\qquad -\Delta y - k^2 y = v \textit{ in } \Omega \left(= \textit{interior of the closure of } \text{of } A \cup \omega\right),$

(3.20) $\qquad (\frac{\partial}{\partial n} - ik + \frac{i}{2k}\Delta_\Gamma)y = 0 \textit{ on } \Gamma,$

and $\mathcal{U}$ defined by

(3.7)′ $\qquad \mathcal{U} = \{v | v \in L^2(\Omega), v = 0 \textit{ in } \omega\}.$

Before computing the gradient J' of J, it is necessary to derive an appropriate *variational formulation* of problem (3.19), (3.20).

The “good” (complex) Hilbert space seems to be defined by

(3.21) $\qquad V = \{z = z_1 + iz_2 | z \in H^1(\Omega), \nabla_\Gamma z \in L^2(\Gamma)\},$

where ∇_Γ is the *tangential gradient* of z on Γ. Multiplying (3.19) by z, and integrating by parts, \
obtain

$$(3.22)\qquad \begin{cases} y \in V;\ \forall z \in V \text{ we have} \\ \int_\Omega \nabla y \cdot \nabla z dx - k^2 \int_\Omega yz dx - i \int_\Gamma (kyz + \frac{1}{2k} \nabla_\Gamma y \cdot \nabla_\Gamma z) d\Gamma = \int_\Omega vz dx. \end{cases}$$

In order to compute the derivative J′ of J, we shall consider (3.19), (3.20) as a system of real valu
equations for the unknown functions y_1 and y_2 such that $y = y_1 + iy_2$, and we shall denote by y tl
pair $\{y_1, y_2\}$. With this notation, equation (3.22) yields(with this time V defined over $\mathbb{R}$)

$$(3.23)\qquad \begin{cases} y \in V \times V;\ \forall z \in V \times V \text{ we have} \\ \int_\Omega \nabla y \cdot \nabla z dx - k^2 \int_\Omega y \cdot z dx + k \int_\Gamma Ry \cdot z d\Gamma + \frac{1}{2k} \int_\Gamma \nabla_\Gamma Ry \cdot \nabla_\Gamma z d\Gamma = \int_\Omega v \cdot z dx, \end{cases}$$

where, in (3.23), $v = \{v_1, v_2\}$ if $v = v_1 + iv_2$, and where the (rotation) matrix R is given by

$$(3.24)\qquad R = \begin{pmatrix} 0 & 1 \\ -1 & 0 \end{pmatrix}.$$

With obvious notation we have

$$(3.25)\qquad J(v) = \frac{1}{2} \int_\gamma |y - g|^2 d\gamma,$$

which implies that

$$(3.26)\qquad \delta J(v) = (J'(v), \delta v) = \int_\gamma (y - g) \cdot \delta y d\gamma.$$

The perturbation δy satisfies (from (3.23))

$$(3.27)\quad \begin{cases} \delta y \in V \times V;\ \forall z \in V \times V \textit{ we have} \\ \int_\Omega \nabla\delta y\cdot\nabla z dx - k^2 \int_\Omega \delta y\cdot z dx + k \int_\Gamma R\delta y\cdot z d\Gamma + \frac{1}{2k}\int_\Gamma \nabla_\Gamma R\delta y\cdot\nabla_\Gamma z d\Gamma \\ = \int_\Omega \delta v\cdot z dx. \end{cases}$$

We introduce now the following *adjoint equation*

$$(3.28)\quad \begin{cases} p \in V \times V;\ \forall z \in V \times V \textit{ we have} \\ \int_\Omega \nabla p\cdot\nabla z dx - k^2 \int_\Omega p\cdot z dx + k \int_\Gamma R^t p\cdot z d\Gamma + \frac{1}{2k}\int_\Gamma \nabla_\Gamma R^t p\cdot\nabla_\Gamma z d\Gamma \\ = \int_\gamma (y - g)\cdot z d\gamma. \end{cases}$$

Taking - as usual - $z = p$ in (3.27) and $z = \delta y$ in (3.28), we obtain that

$$\delta J(v) = \int_\Omega p \cdot \delta v dx,$$

which implies in turn that

$$(3.29)\quad (J'(v), w) = \int_\Omega p \cdot w dx,\ \forall w \in L^2(\Omega) \times L^2(\Omega).$$

If $\mathcal{U}$ is defined by (3.7)$'$ we can identify $J'(v)$ to $p|_A$.

Using the knowledge of J' we can solve the control problem (3.17) by either conjugate gradient or GMRES algorithms operating in the space $\mathcal{U}$. The conjugate gradient algorithm is indeed an (almost) straightforward variation of algorithm (2.17)-(2.29) of Section 2.2.3; however due to the importance of the problem under consideration the conjugate gradient solution of the control problem (3.17) will be described in the following Section 3.4.2.

3.4.2 Conjugate gradient solution of the control problem (3.17).

We use the vector formulation of the control problem (3.17) (see Sec. 3.4.1) and define $\mathcal{U}$ by

(3.30) $\mathcal{U} = \{v | v \in L^2(\Omega) \times L^2(\Omega),\ v = 0 \text{ on } \omega\}$

(the functions in (3.30) are now real valued).

The conjugate gradient algorithm is defined as follows:

Initialization:

(3.31) $u^o \in \mathcal{U}$ *is given;*

solve the variational Helmholtz equations

$$(3.32)\quad \begin{cases} y^o \in V \times V, \\ \int_\Omega \nabla y^o \cdot \nabla z dx - k^2 \int_\Omega y^o \cdot z dx + k \int_\Gamma R y^o \cdot z d\Gamma + \frac{1}{2k} \int_\Gamma \nabla_\Gamma R y^o \cdot \nabla_\Gamma z d\Gamma \\ = \int_A u^o \cdot z dx,\ \forall z \in V \times V, \end{cases}$$

and

$$(3.33)\quad \begin{cases} p^o \in V \times V, \\ \int_\Omega \nabla p^o \cdot \nabla z dx - k^2 \int_\Omega p^o \cdot z dx + k \int_\Gamma R^t p^o \cdot z d\Gamma + \frac{1}{2k} \int_\Gamma \nabla_\Gamma R^t p^o \cdot \nabla_\Gamma z d\Gamma \\ = \int_\gamma (y^o - g) \cdot z d\gamma,\ \forall z \in V \times V. \end{cases}$$

Define

(3.34) $g^o = p^o \chi_A$

and

(3.35) $\mathbf{w}^o = \mathbf{g}^o$. □

Then, for n $\geq$ 0, *assuming that* $\mathbf{u}^n$, $\mathbf{y}^n$, $\mathbf{g}^n$ *and* $\mathbf{w}^n$ *are known we update them as follows:*

Descent:

Solve

$$(3.36)\quad \begin{cases} \bar{\mathbf{y}}^n \in V \times V, \\ \int_\Omega \nabla\bar{\mathbf{y}}^n \cdot \nabla \mathbf{z} dx - k^2 \int_\Omega \bar{\mathbf{y}}^n \cdot \mathbf{z} dx + k \int_\Gamma R\bar{\mathbf{y}}^n \cdot \mathbf{z} d\Gamma + \frac{1}{2k}\int_\Gamma \nabla_\Gamma \bar{\mathbf{y}}_n \cdot \nabla_\Gamma \mathbf{z} d\Gamma] \\ = \int_A \mathbf{w}^n \cdot \mathbf{z} dx, \ \forall \mathbf{z} \in V \times V, \end{cases}$$

and

$$(3.37)\quad \begin{cases} \bar{\mathbf{p}}^n \in V \times V, \\ \int_\Omega \nabla\bar{\mathbf{p}}^n \cdot \nabla \mathbf{z} dx - k^2 \int_\Omega \bar{\mathbf{p}}^n \cdot \mathbf{z} dx + k \int_\Gamma R^t\bar{\mathbf{p}}^n \cdot \mathbf{z} d\Gamma + \frac{1}{2k}\int_\Gamma \nabla_\Gamma R^t \bar{\mathbf{p}}^n \cdot \nabla_\Gamma \mathbf{z} d\Gamma \\ = \int_\gamma \bar{\mathbf{y}}^n \cdot \mathbf{z} d\gamma, \ \forall \mathbf{z} \in V \times V. \end{cases}$$

Compute then

$$(3.38)\quad \rho_n = \frac{\int_A |\mathbf{g}^n|^2 dx}{\int_A \mathbf{p}^n \cdot \mathbf{w}^n dx},$$

and

$$(3.39)\quad \mathbf{u}^{n+1} = \mathbf{u}^n - \rho_n \mathbf{w}^n,$$

$$(3.40)\quad \mathbf{y}^{n+1} = \mathbf{y}^n - \rho_n \bar{\mathbf{y}}^n,$$

(3.41) $$g^{n+1} = g^n - \rho_n \overline{p}^n \chi_A.$$

Testing the convergence and constructing the new descent direction:

If $\|g^{n+1}\|_{\mathcal{U}}/\|g^o\|_{\mathcal{U}} \leq \epsilon$ *take* $u = u^{n+1}$ *and* $y = y^{n+1}$; *if not compute*

(3.42) $$\gamma_n = \frac{\int_A |g^{n+1}|^2 dx}{\int_A |g^n|^2 dx},$$

and

(3.43) $$w^{n+1} = g^{n+1} + \gamma_n w^n. \qquad \square$$

Do n=n+1 *and go to* (3.36).

The implementation of algorithm (3.31)-(3.43) requires the solution at each iteration of two Helmholtz problems associated to a bilinear form which is neither symmetric nor coercive. In the practical implementation of the above algorithm we advocate, among other techniques a GMRES algorithm like the one discussed in [11, pp. 213-216] using as fundamental Hilbert space the space V×V equipped with the following scalar product

(3.44) $$(y,z)_{V\times V} = \int_\Omega (\nabla y\cdot\nabla z + k^2 y\cdot z)dx + \int_\Gamma (ky\cdot z + \frac{1}{2k}\nabla_\Gamma y\cdot\nabla_\Gamma z)d\Gamma.$$

The elliptic operator associated to the scalar product (3.44) will act as a preconditioner. More details concerning the practical implementation of algorithm (3.31)-(3.43) and of the associated GMRES solvers will be given in [12].

For an introduction to GMRES algorithms see, e.g. [13], and for application in Computational Chemistry (Schrödinger equation) see [14].

4. Numerical Experiments

The fictitious domain methods described in Sections 2 and 3 have been applied to the solution of Dirichlet, Neumann and Helmholtz problems when A is a disk, a sphere or an ellipsoïd.

4.1 Application to the solution of an exterior Dirichlet problem in two-dimensions.

For this test case, A is a disk of radius .5, imbedded in a square whose edges are of length 6 and whose centroïd coincides with the disk center. Dirichlet conditions have been prescribed on ∂A and on the exterior boundary Γ. Figures 4.1 and 4.2 show a comparison between the exact (•) and computed (Δ) solutions on a line which is almost a diameter; Figure 4.1 (resp. 4.2) corresponds to 400 (resp. 2500) grids points in Ω and 10 (resp. 52) control points in A. The results are reasonable for the coarse mesh and very good for the fine one.

Remark 4.1. The interesting part of the solution, on Figures 4.1 and 4.2, is the one for which x lies outside the interval $(-\frac{1}{2}, \frac{1}{2})$.

4.2 Applications to the solution of an exterior Neumann problem in two-dimensions.

This test case is quite close to the above one; here we have a Neumann condition on ∂A and a Dirichlet one on the exterior boundary Γ, with A and Ω as in Section 4.1.

The numerical results are shown on Figures 4.3 (coarse grid) and 4.4 (fine grid), with the numbers of grid and controls points as in Section 4.1. Despite the greater difficulty of the Neumann problem compared to Dirichlet's the results are quite good, in particular for the fine grid, despite the fact that the number of control points is not very large (52).

Remark 4.1 still holds for Figures 4.3 and 4.4.

4.3 Application to the Helmholtz equation

We compute the scattered field on a sphere and an ellipsoïd using the methodology discussed in Section 3 for solving the Helmholtz equation. The boundary condition on the obstacle A is of Dirichlet type while the one on Γ is the absorbing boundary condition (3.13). The first case concerns the calculation of the field scattered by a sphere of radius R=.25m, with the wavelength λ=.26m, the coefficient k in (3.1), (3.30) being 24.16 (the corresponding frequency is 1.15 Ghz). The mesh size used for the calculation has been $h=\frac{\lambda}{6}, \frac{\lambda}{10}, \frac{\lambda}{15}$, with the artificial boundary Γ located at a distance $\frac{\lambda}{2}$ from the body. The total number of grid points is $45^3 = 91{,}125$. Figures 4.5, 4.6, 4.7 show, the computed and exact scattered fields as functions of the polar angle θ in the horizontal plane. As shown by Figure 4.7 computed and exact solutions compare quite favorably when $h=\frac{\lambda}{15}$.

In the second test case, the scattering body is an ellipsoïd whose principal axes are parallel to the coordinate directions, the corresponding diameters being 2λ, 2λ and 4λ (the ellipsoïd is axisymmetric).

For the two calculations presented below we have taken $h=\lambda/10$, the artificial boundary Γ being located at a distance $.7\lambda$ from A. In Ω, we used a mesh of $35\times35\times35=67{,}375$ grid points.

In Figures 4.8 and 4.9, we show a computed solution of the scattered far field via the RSC diagram. Figure 4.8 (resp. 4.9) corresponds to the situation where the "illuminating" field corresponds to a plane wave propagating vertically (resp. horizontally), the diagram of Figure 4.8 (resp. 4.9) being made in a vertical (resp. horizontal) plane. As we can see from Figures 4.8 and 4.9 the computed solution is quite accurate despite the fact that the artificial boundary Γ is close to the body A.

Finally, on Figure 4.10 we have shown the variation of the residual in the GMRES algorithm, versus the number of iterations.

5. Conclusion

Combining control methods to fictitious domain strategies seems to provide an interesting alternative to standard approximations using non structured grids to describe accurately non regular geometries. Despite the large amount of work already done in these directions, we still think that there is room for many improvements concerning for example the preconditioning of the iterative method of solution and also the control criteria and approximations issues to maintain the quality of the approximation in the neighborhood of the physical boundary.

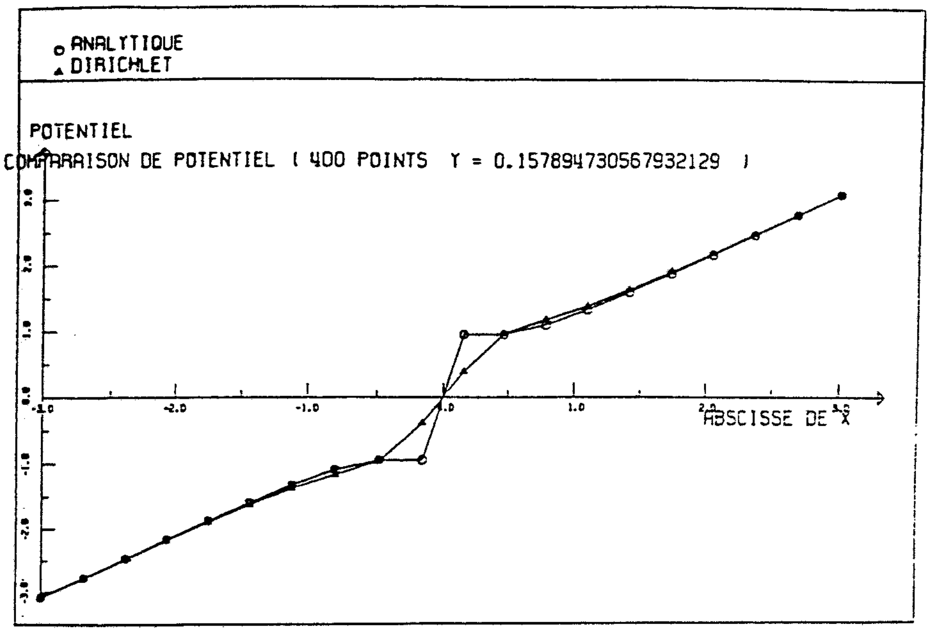

Figure 4.1

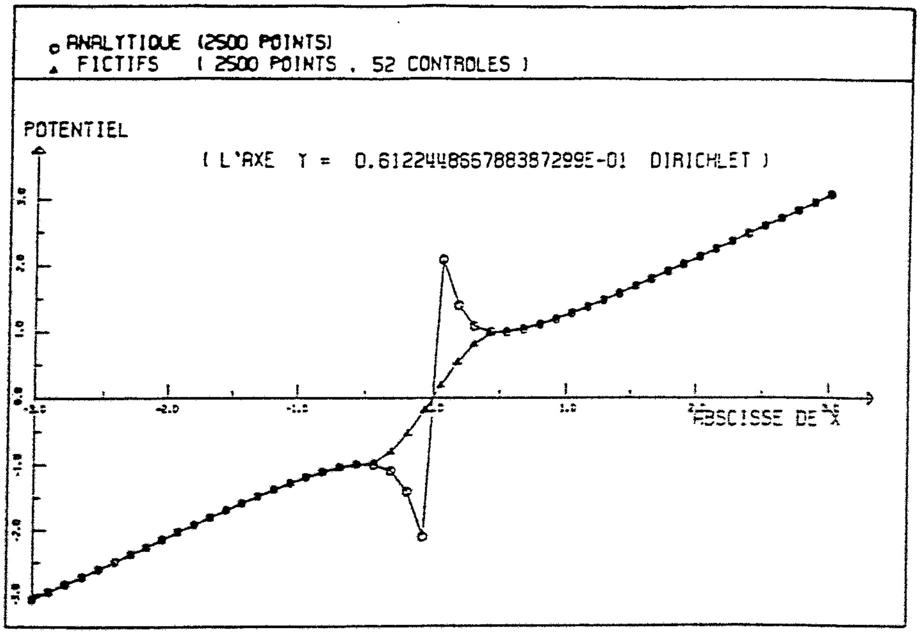

Figure 4.2

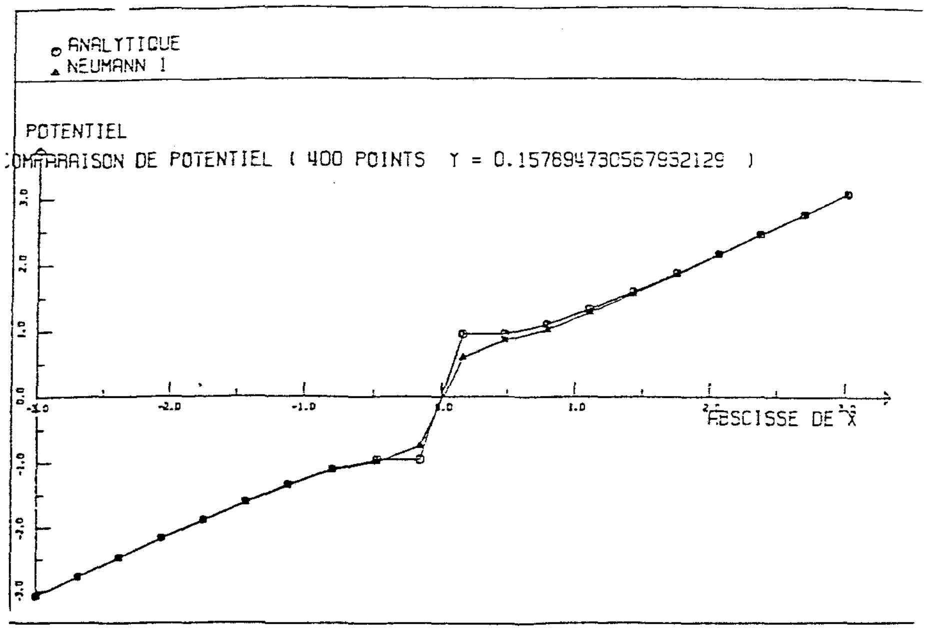

Figure 4.3

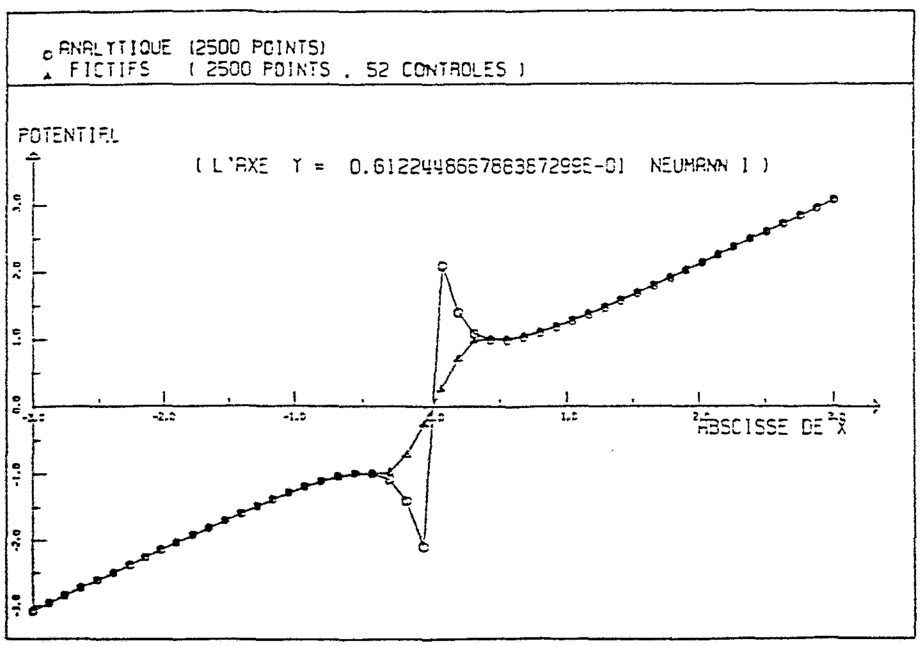

Figure 4.4

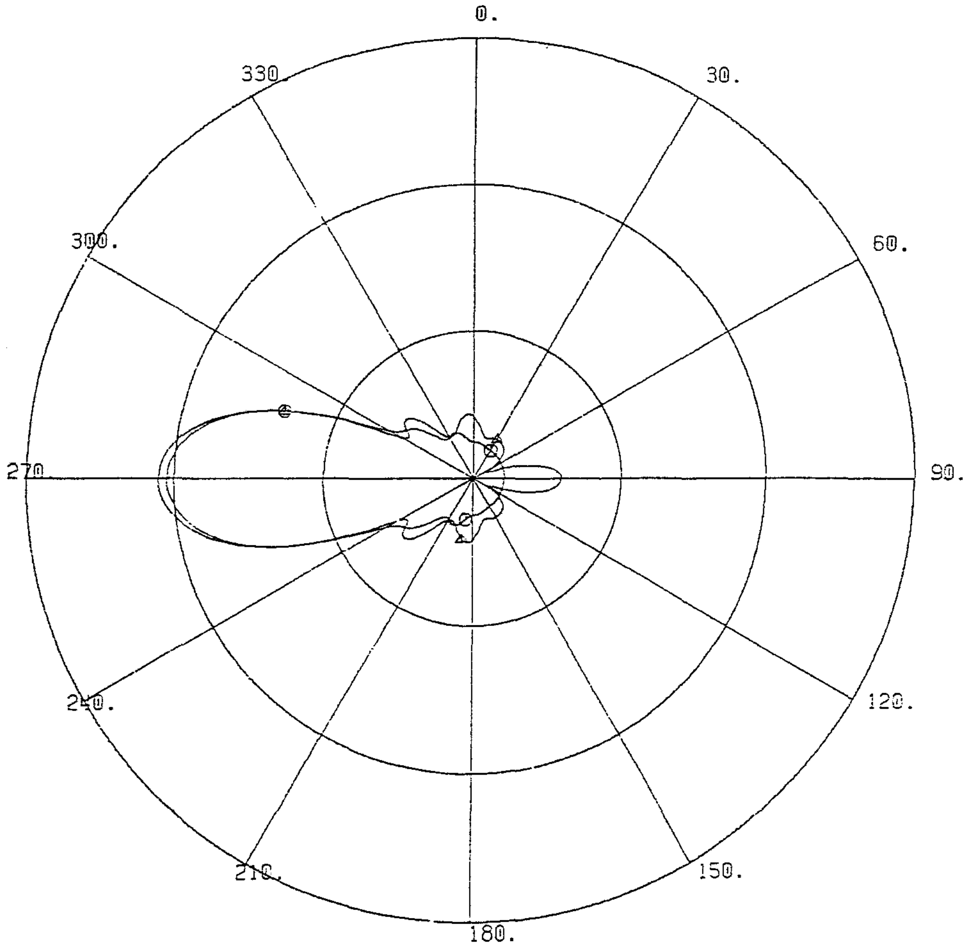

$h = \lambda/6$, • = exact solution

Δ = computed solution

DB -20.0 -10.0 0.0 10.0

Figure 4.5

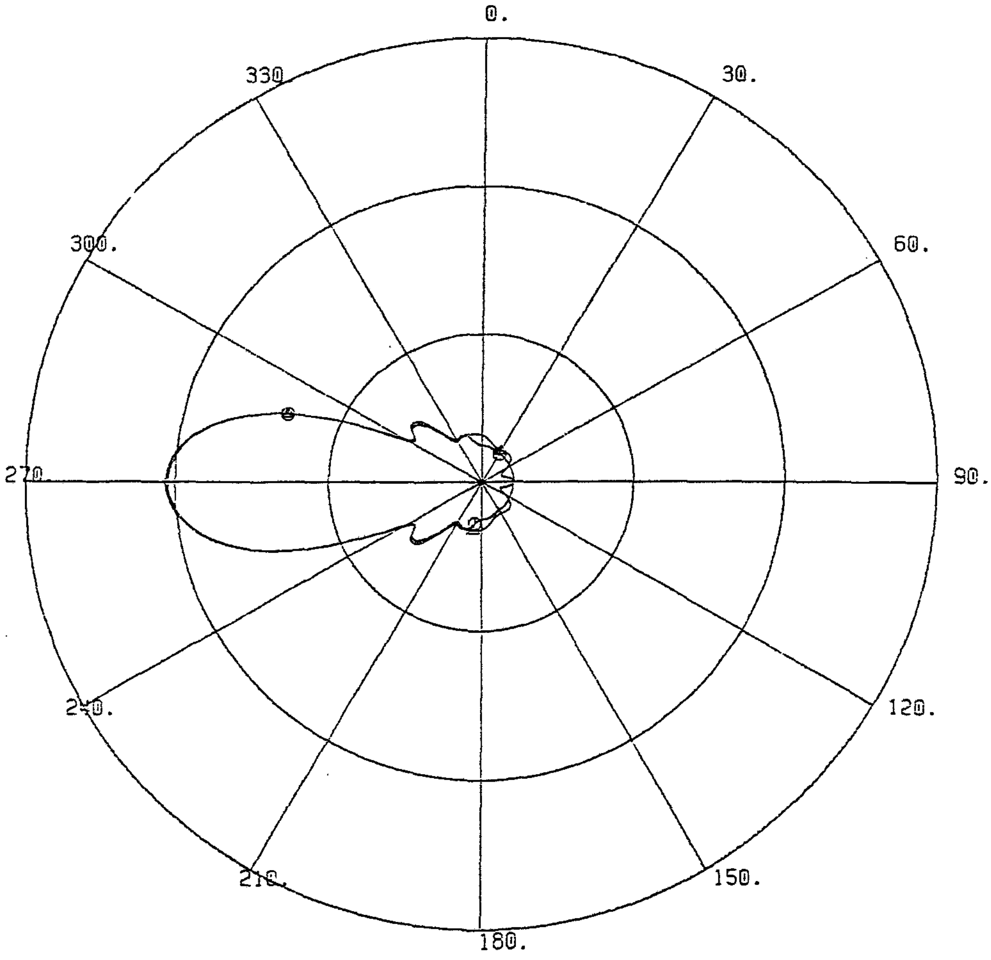

$h = \lambda/10$, • = exact solution

Δ = computed solution

DB -20.0 -10.0 0.0 10.0

Figure 4.6

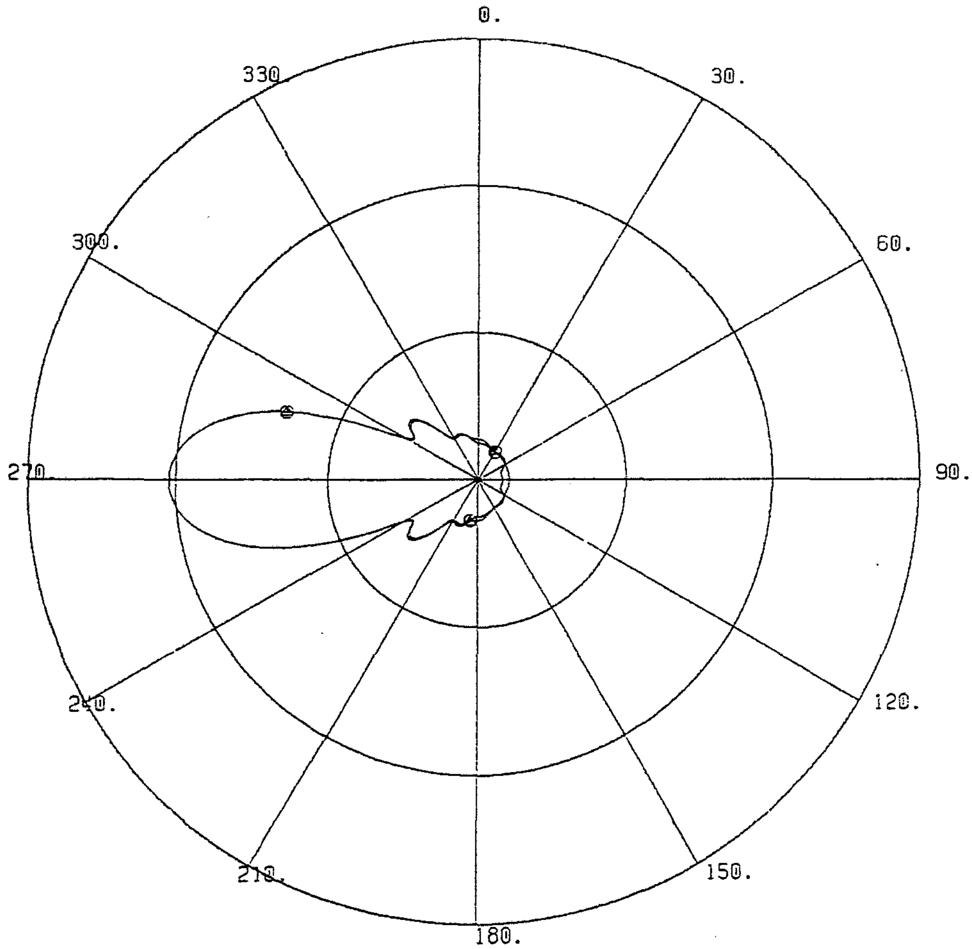

$h = \lambda/15$, • = exact solution

Δ = computed solution

DB -20.0 -10.0 0.0 10.0

Figure 4.7

• =computed solution.

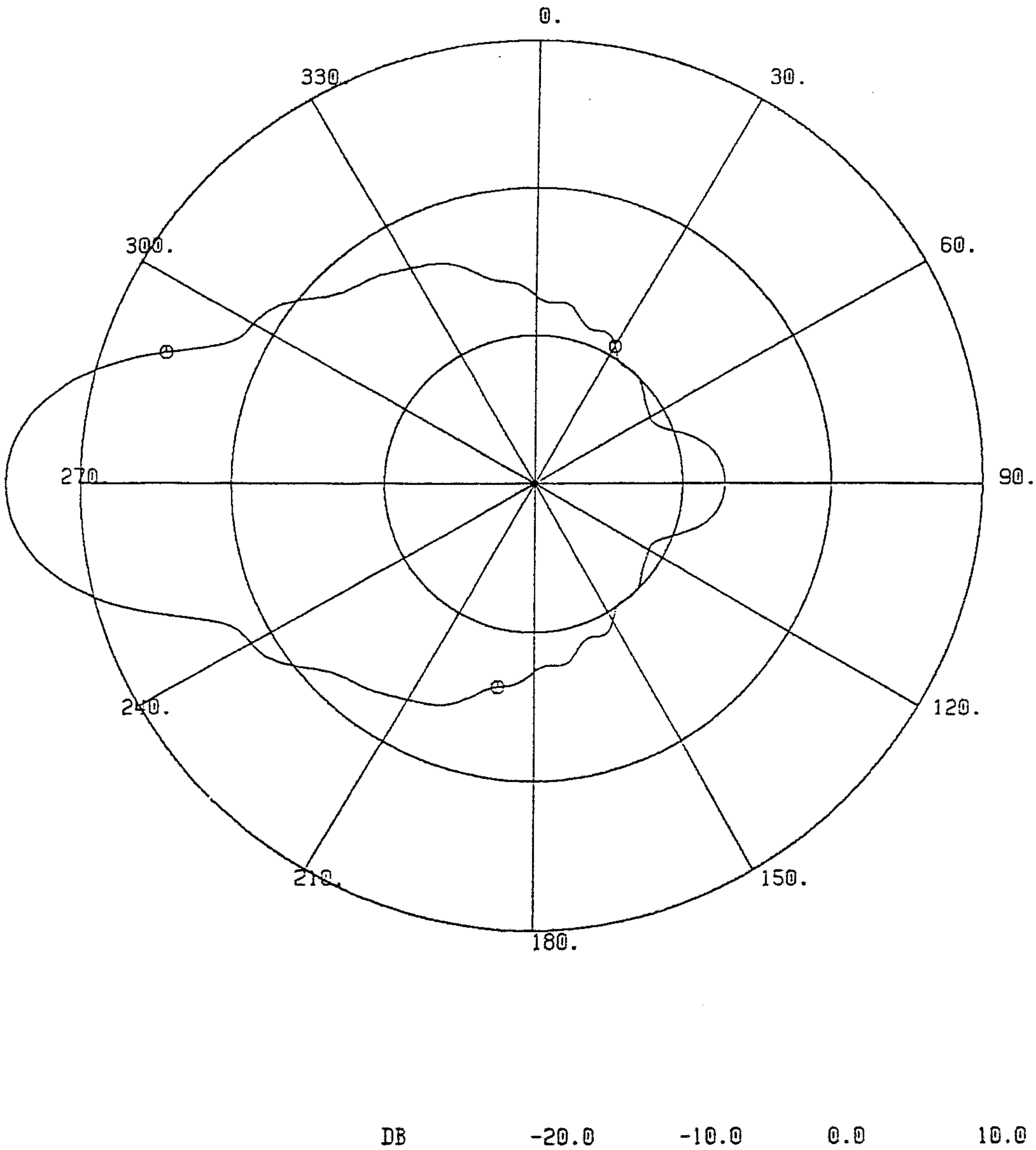

Figure 4.8

• =computed solution.

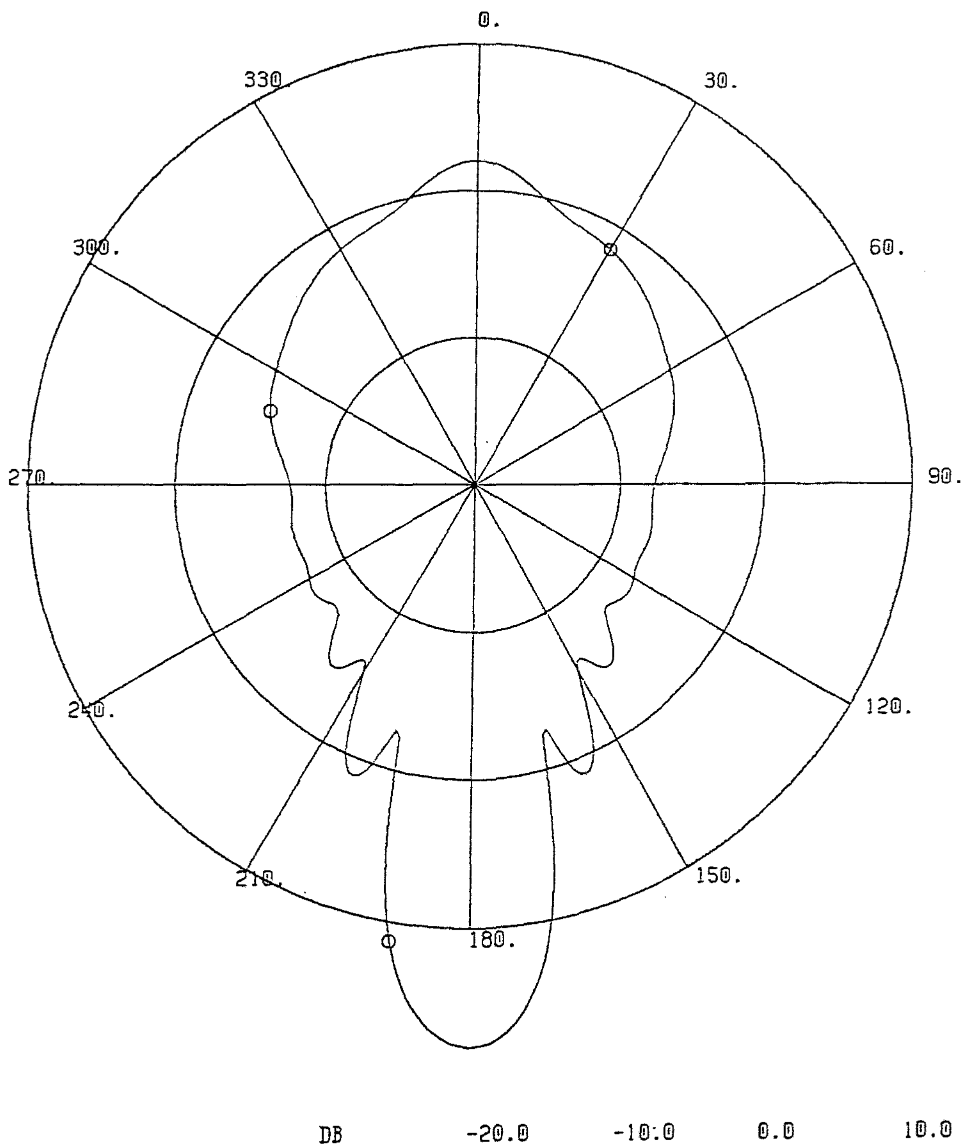

Figure 4.9

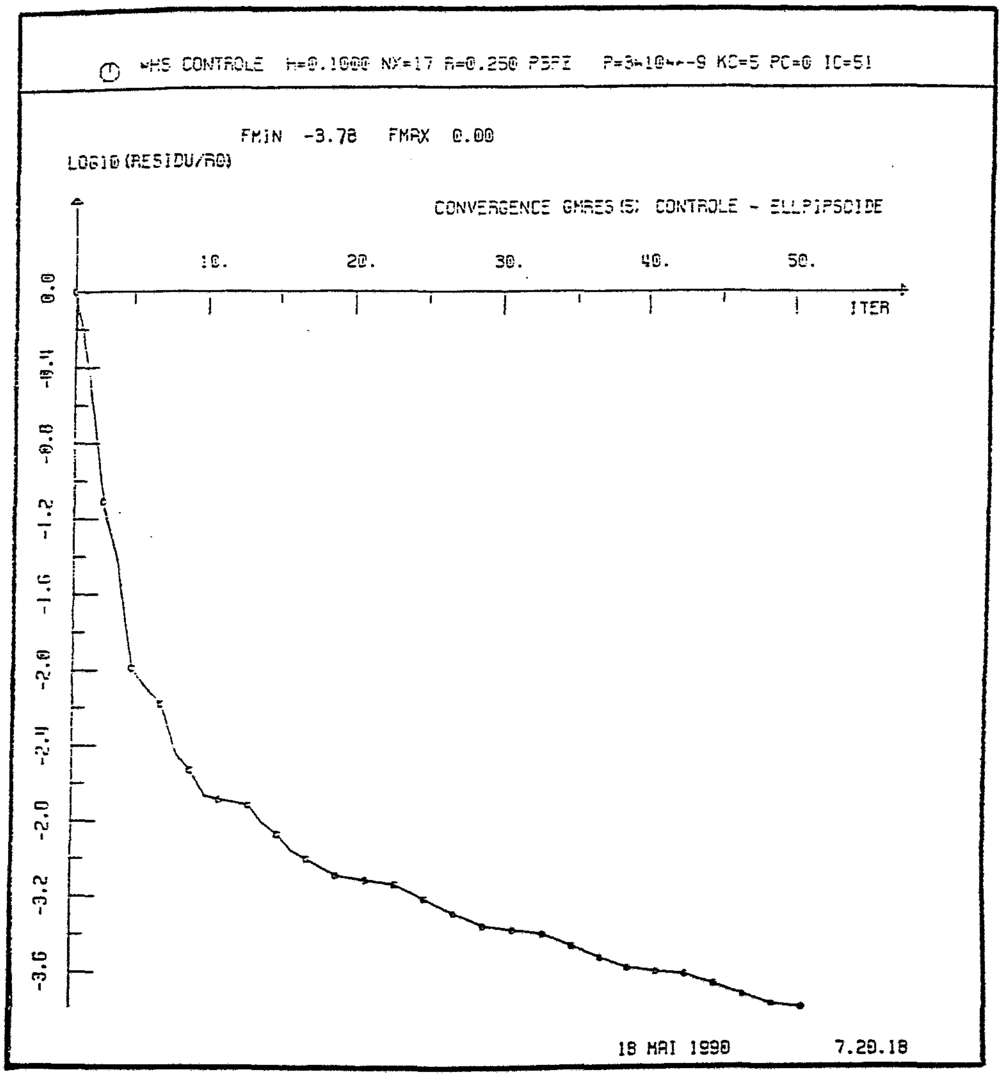

Figure 4.10

Acknowledgments

The authors would like to thank P. L. Lions, H. Steve, P. Joly for helpful comments and suggestions. The support of NSF, via NSF Grants # INT-8612680 and DMS-8822522 and of DRET, via Grant # 89424, is also acknowledged. We would also like to thank Juana A. Wilson for her processing of this paper.

References

[1] G. P. ASTRAKMANTSEV, Methods of fictitious domains for a second order elliptic equation with natural boundary conditions, *U.S.S.R. Computational Math. and Math. Phys.*, 18 (1978), pp. 114-121.

[2] G. I. MARCHUK, Y. A. KUZNETSOV, A. M. MATSOKIN, Fictitious domain and domain decomposition methods, *Sov. J. Num. Anal. Math. Modelling*, 1 (1986), pp. 3-35.

[3] S. A. FINOGENOV, Y. A. KUZNETSOV, Two-stage fictitious component methods for solving the Dirichlet boundary value problem, *Sov. J. Num. Anal. Math. Modelling*, 3 (1988), pp. 301-323.

[4] W. PROSKUROWSKI, O. WIDLUND, On the numerical solution of Helmholtz equation by the capacitance matrix method, *Math. Comp.*, 30 (1979), pp. 433-468.

[5] D. P. O'LEARY, O. WIDLUND, Capacitance matrix methods for the Helmholtz equation on general three-dimensional regions, *Math. Comp.*, 3 (1979), pp. 849-879.

[6] D. P. YOUNG et al, A locally refined rectangular grid finite element method (to appear in *Journal of Computational Physics*).

[7] J. L. LIONS, *Contrôle Optimal des systèmes gouvernés par des équations aux dérivées partielles*, Dunod, Paris, 1969.

[8] R. GLOWINSKI, Lagrange multiplier, optimal control and fictitious domains methods (to appear).

[9] B. ENGQUIST, A. MAJDA, Absorbing boundary conditions for the numerical computation of waves, *Math. Comp.*, 31, (1977), pp. 629-651.

[10] B. ENGQUIST, A. MAJDA, Radiation boundary conditions for accoustic and elastic wave calculations, *Comm. Pure Appl. Math.*, 32, (1979), pp. 313-357.

[11] M. O. BRISTEAU, R. GLOWINSKI, J. PERIAUX, Acceleration procedures for the numerical simulation of compressible and incompressible viscous flows in *Advances in Computational Nonlinear Mechanics*, I. S. Doltsinis ed., Springer-Verlag, Wien, 1989, pp. 197-243.

[12] C. ATAMIAN, *Numerical methods for Helmholtz and Maxwell equations by fictitious domain methods*, Thesis (to appear).

[13] Y. SAAD, M. H. SHULTZ, GMRES: A generalized minimal residual algorithm for solving non symmetric linear systems, *SIAM J. Sci. Stat. Comp.*, 7, (1986), pp. 856-

[14] R. WYATT et al, Lecture at the Ninth International Conference on Computing Methods in Applied Sciences and Engineering, Paris, February 1990.